# *Deciphering the intermodel spread in projections of the impacts of Indian summer monsoon on ENSO under global warming*



Lin, S. ORCID: https://orcid.org/0000-0003-0809-7911, Yang, S. ORCID: https://orcid.org/0000-0001-8345-8583, Dong, B. ORCID: https://orcid.org/0000-0003-0809-7911, Deng, K. ORCID: https://orcid.org/0000-0002-6510-8181 and Fang, K. (2025) Deciphering the intermodel spread in projections of the impacts of Indian summer monsoon on ENSO under global warming. Journal of Geophysical Research: Atmospheres, 130 (4). e2024JD042803. ISSN 2169-8996 doi: 10.1029/2024JD042803 Available at https://centaur.reading.ac.uk/121249/

JGR Atmospheres

RESEARCH ARTICLE
10.1029/2024JD042803

# Deciphering the Intermodel Spread in Projections of the Impacts of Indian Summer Monsoon on ENSO Under Global Warming

**Shuheng Lin[1], Song Yang[2,3], Buwen Dong[4], Kaiqiang Deng[2,3], and Keyan Fang[1]**

[1]Key Laboratory of Humid Subtropical Eco-geographical Process (Ministry of Education), College of Geographical Sciences, Fujian Normal University, Fuzhou, China, [2]School of Atmospheric Sciences, Sun Yat-sen University, Southern Marine Science and Engineering Guangdong Laboratory (Zhuhai), Zhuhai, China, [3]Guangdong Province Key Laboratory for Climate Change and Natural Disaster Studies, Sun Yat-sen University, Zhuhai, China, [4]National Centre for Atmospheric Science, Department of Meteorology, University of Reading, Reading, UK

**Abstract** The Indian summer monsoon (ISM) is intricately linked to the El Niño-Southern Oscillation (ENSO) on interannual timescale. Although previous studies have explored ENSO's effects on the ISM, the reverse influence, particularly under global warming, remains unclear. This study examines the projected changes in the ISM's impacts on ENSO under the SSP5-8.5 emission scenario using 34 climate models from the Coupled Model Intercomparison Project Phase 6 (CMIP6) that reasonably simulate the monsoon's effects on ENSO. A significant spread is found in the projections across the models, with approximately half of the models projecting an enhancing influence of ISM on ENSO, whereas the other half indicates a weakening effect. The intermodel spread is primarily associated with the projected changes in the strength of the feedback between precipitation and low-level circulation over the tropical northwest Pacific, which is crucial for generating ISM-induced anomalous circulation over the region. Models projecting an enhanced precipitation-circulation feedback simulate larger ISM-driven rainfall and circulation anomalies over the tropical northwest Pacific in a warmer climate, leading to more pronounced zonal wind anomalies near the equator along the southern side of the anomalous circulation and vice versa. As a result, the larger zonal wind anomalies caused by abnormal monsoons exert intensified effects on the subsequent ENSO evolution by significantly suppressing or amplifying the atmosphere-ocean coupling processes related to ENSO development.

**Plain Language Summary** The Indian summer monsoon and the El Niño-Southern Oscillation (ENSO) are two important climate systems that drastically influence regional and global climate variations. Their interaction contributes significantly to the year-to-year variability of both the systems and their climate impacts. The responses of ENSO and its influences on monsoon to global warming have been investigated extensively; however, the potential changes in the monsoon's impacts on ENSO are less understood. In this work, 34 climate models within the Coupled Model Intercomparison Project Phase 6 are analyzed to investigate how the monsoon's effects on ENSO may change in a warmer future. Results reveal a large diversity in the projections across the models. About half of these models simulate that the monsoon will exert stronger effects on ENSO evolution under global warming, but the rest suggest an opposite change. This variation among models mainly results from the differences in how they project the changes in the strength of feedback between precipitation and low-level circulation over the tropical northwest Pacific. This finding is helpful for enhancing our understanding of the uncertainties in future projections of ENSO-monsoon relationships.

**Key Points:**

- Projections in the impacts of Indian summer monsoon (ISM) on ENSO under global warming show a large spread among CMIP6 models
- The intermodel spread is primarily caused by the diverse changes in precipitation-circulation feedback over the tropical northwest Pacific
- Models with strengthening feedback project an enhancing ISM influence on ENSO, while those with weakening feedback suggest a reducing effect

**Supporting Information:**

Supporting Information may be found in the online version of this article.

**Correspondence to:**

S. Yang,
yangsong3@mail.sysu.edu.cn

**Citation:**

Lin, S., Yang, S., Dong, B., Deng, K., & Fang, K. (2025). Deciphering the intermodel spread in projections of the impacts of Indian summer monsoon on ENSO under global warming. *Journal of Geophysical Research: Atmospheres*, *130*, e2024JD042803. https://doi.org/10.1029/2024JD042803

Received 25 OCT 2024
Accepted 25 JAN 2025



## 1. Introduction

The Indian summer monsoon (ISM) is a crucial component of the broader Asian summer monsoon system. It brings substantial moisture to India and surrounding regions, significantly affecting the livelihoods of billions of people and the economic progress in many countries (Chowdary et al., 2021; Fang et al., 2024; S. Yang et al., 2024). The interannual variation of the ISM is closely linked to the El Niño-Southern Oscillation (ENSO), a coupled atmosphere-ocean phenomenon in the tropical Pacific that significantly influences regional to global climate (J. Chen et al., 2024; S. Yang, Li, et al., 2018; Zhang et al., 1996). ISM rainfall typically becomes below average during the El Niño developing summer while it tends to be above normal during La Niña events (Rasmusson & Carpenter, 1983; B. Wang et al., 2001; Webster & Yang, 1992), leading to a negative simultaneous correlation between monsoon and ENSO (Kumar et al., 1999; Yasunari, 1990). The anomalous sea surface

temperatures (SST) warming in the equatorial central-eastern Pacific associated with El Niño can trigger an anomalous Walker circulation, which induces anomalous downward motions and thus reduces rainfall over India (Ju & Slingo, 1995; Kumar et al., 2006).

The influences of ISM on ENSO have also been discussed previously (e.g., Nigam, 1994; Webster & Yang, 1992; Yasunari, 1990; S. Yang, Deng & Duan, 2018). The strongest negative lagged correlation between ENSO and ISM rainfall is observed when ENSO SST anomalies follow the ISM rainfall by 3–6 months, implying a potential role of anomalous ISMs in modulating the following ENSO evolution (Lau & Yang, 1996; Webster & Yang, 1992; Yasunari, 1990). Additionally, it has been argued that a weak ISM can promote the development of El Niño events and inhibit that of La Niña events, whereas a strong ISM tends to have an opposite effect (Lin et al., 2023; R. Wu & Kirtman, 2003). These findings from statistical analyses align with the results of sensitivity experiments conducted using simple or fully coupled models (Chung & Nigam, 1999; Kirtman & Shukla, 2000; Lin et al., 2023; Meehl, 1997; Nigam, 1994). Lin et al. (2023) shed further light on the physical mechanisms underlying the monsoon's effects on ENSO evolution. A strong monsoon can lead to reduced rainfall and anomalous anticyclonic circulation over the tropical northwest Pacific (NWP). The anomalous easterly wind on the southern side of the anticyclonic circulation can influence the subsequent ENSO development via triggering upwelling Kelvin waves and westward movement of cold seawater.

The changes in ENSO-ISM relationship in response to global warming have been widely examined; however, a consensus has yet to be achieved. Based on observational data sets, previous studies have found a considerable weakening in the simultaneous correlation between the ISM and ENSO after the 1970s (Kinter et al., 2002; Kumar et al., 1999) followed by a clear restoration of this relationship since 2000 (X. Yang & Huang, 2021). However, the limited length of observations makes it difficult to determine whether these changes are driven by internal variability or anthropogenic forcing. Climate models have been utilized to explore how the ENSO-ISM connection might change under global warming. For instance, Annamalai et al. (2007), using CMIP3 models that successfully simulated the lead-lag correlation between ISM and ENSO, showed that although both the mean state and the interannual variability of ISM rainfall were expected to increase under $CO_2$ doubling scenarios, the ENSO-monsoon linkage was not projected to diminish as global temperatures rise. In contrast, several studies analyzing experiments of high emission scenarios in CMIP5 models (Li & Ting, 2015) or the idealized 1pctCO2 experiment of the NCAR climate model (Goswami & An, 2022) have indicated a potential weakening of the simultaneous correlation between ENSO and ISM. However, Aneesh and Bódai (2024) argued that the changes in this correlation were not robustly modeled at the end of the 21st century resulting from the diverse changes in ENSO amplitude among the CMIP models. These studies highlight the ongoing debate regarding how the ENSO-ISM relationship will respond to a warmer climate with a primary focus on the ENSO impacts on ISM. However, how the ISM influences ENSO under global warming remains underexplored. Investigating the potential changes in the monsoon's impact on ENSO may help clarify the uncertainties in projections of their relationship.

This study utilizes 34 CMIP6 models that exhibit reliable performance in capturing the impacts of ISM on ENSO to investigate the projections of ISM influences on ENSO under global warming and to identify the major causes of the intermodel spread in these projections. The structure of this paper is as follows: the data sets and methodology are presented in Section 2. Section 3 investigates the projected changes in the ISM's impacts on ENSO under global warming, and the primary cause of intermodel uncertainty in the projections is examined in Section 4. Section 5 provides conclusions and discussion.

## 2. Data and Methods

### 2.1. Data Sets

This study uses the monthly mean outputs from the historical and shared socioeconomic pathway 5–8.5 (SSP585) simulations of 40 CMIP6 models (Eyring et al., 2016) as summarized in Table S1 in Supporting Information S1. The first realization ("r1i1p1f1") is analyzed for the majority of the models while using alternative realizations in the models where "r1i1p1f1" is not available for the historical or SSP585 simulations (Table S1 in Supporting Information S1). To ensure an adequate sample size for the composite analysis, a long period of historical simulations (1900–2014) is analyzed and defined as the historical climate, whereas the SSP585 simulations covering 2015 to 2099 are considered projections of a future warmer climate. All model outputs are re-gridded into a uniform 2.5° × 2.5° horizontal resolution. Monthly observational data sets are employed to evaluate model performance, including the monthly SST data of the Hadley Center Sea Ice and SST (HadISST), with a 1° × 1°

resolution spanning 1870–present (Rayner et al., 2003), and the all-India monthly rainfall (AIMR) provided by the Indian Institute of Tropical Meteorology from 1871 to 2016 (Parthasarathy et al., 1994).

### 2.2. Methods

Anomaly fields are derived by removing the linear trend and climatological seasonal cycle and then filtered using a sixth-order 4–108 months Butterworth band-pass filter to isolate interannual variability. The anomaly fields in both the historical and SSP585 simulations are calculated with reference to the climatology of the respective experiments. ENSO intensity is measured by the Niño3.4 (170°W–120°W, 5°S–5°N) SST anomaly in both observations and CMIP6 models. Seasonal mean AIMR during June–September (JJAS) is utilized to depict the observed ISM variability, and the JJAS-mean rainfall anomaly averaged over the region of 70°E−90°E, 10°N–30°N is applied to denote the monsoon rainfall variation in the CMIP6 models. The statistical significance of regression and correlation coefficients is calculated based on the Student's *t*-test. Following previous studies (Lin et al., 2024a; Power et al., 2012), the multimodel ensemble mean (MME) of changes in variable anomalies is deemed significant when more than 68% of the models exhibit the same sign as the MME.

Following the prior studies (Lin et al., 2023, 2024b; R. Wu & Kirtman, 2003), a conditional classification approach is applied to depict the ISM's effects on ENSO evolution. By comparing the JJAS mean Niño3.4 index with its 0.43 standard deviation (STD), specific years are determined as El Niño, La Niña, or ENSO-neutral years, respectively. Likewise, we determine whether an ISM year is anomalous or normal by comparing the JJAS-mean monsoon rainfall anomaly to its STD. A threshold of 0.43 STD is applied to ensure that the three categories for both ENSO and ISM years contain nearly equal numbers of events, since the Niño3.4 index and ISM rainfall anomalies exhibit a roughly normal distribution with a mean of zero. Using this conditional framework, El Niño (La Niña) years are further grouped by their co-occurrence with a strong, weak, or normal monsoon, defined as EN (LN)-Wet, EN (LN)-Dry, and EN (LN)-Nor years, respectively (Table S2 in Supporting Information S1). Comparing the composite values of ENSO years coinciding with a weak or strong ISM and those with a normal ISM highlights the potential impacts of monsoon on ENSO. We also perform the same classification and composite analyses based on the December–February Niño3.4 index with the primary results remaining consistent.

It has been reported that some CMIP6 models fail to simulate the significant impacts of ISM on ongoing ENSO evolution (Lin et al., 2024b). Following Lin et al. (2024b), we evaluate the ability of 40 CMIP6 models to represent the correlations between JJAS ISM rainfall and the monthly Niño3.4 index during the following OND by comparing the values in observations and the historical simulations (Figure S1a in Supporting Information S1). Although most CMIP6 models simulate weaker ISM-ENSO correlation compared to observations, 34 models show statistically significant correlations at the 99% confidence level and are thus classified as good-performance models (GPMs). By contrast, the remaining six models fail to simulate a significant negative correlation with two even simulating an opposite sign. We refer to these 6 models as bad-performance models (BPMs). The GPMs successfully simulate the general characteristics of the evolution of lagged correlations between the Niño3.4 index and ISM rainfall (Figure S1b in Supporting Information S1). That is, the strongest negative correlation appears in the OND following the monsoon season. By contrast, the BPMs show poor skill in reproducing the timing of the ENSO-ISM association.

To further examine the performance of GPMs and BPMs in representing the ISM's impacts on ENSO evolution, we analyze the monthly evolution of Niño3.4 index during the categorized ENSO events (Figure S2 in Supporting Information S1). Indeed, the GPMs reasonably reproduce the influence of abnormal monsoons on the following ENSO development. A weak monsoon tends to strengthen the development of an ongoing El Niño event while to weaken that of a La Niña event, whereas a strong monsoon shows opposite features. In contrast, the BPMs show much smaller differences in wintertime Niño3.4 index between ENSO events accompanied by an abnormal monsoon and those with a normal monsoon. A weak monsoon even exerts reversed influences on ENSO compared to the observations. Overall, these results indicate that the 34 CMIP6 models can reproduce the effects of ISM on subsequent ENSO progress, whereas the remaining six models fail to do so. To lessen the potential effect of model biases on future projections, we focus on the 34 models with relatively good performance to investigate the projected changes in the ISM's impacts on ENSO.

To quantify the projected change in influences of ISM on subsequent ENSO evolution, we define an index based on the composite differences in SST anomaly between ENSO events coinciding with an abnormal monsoon and

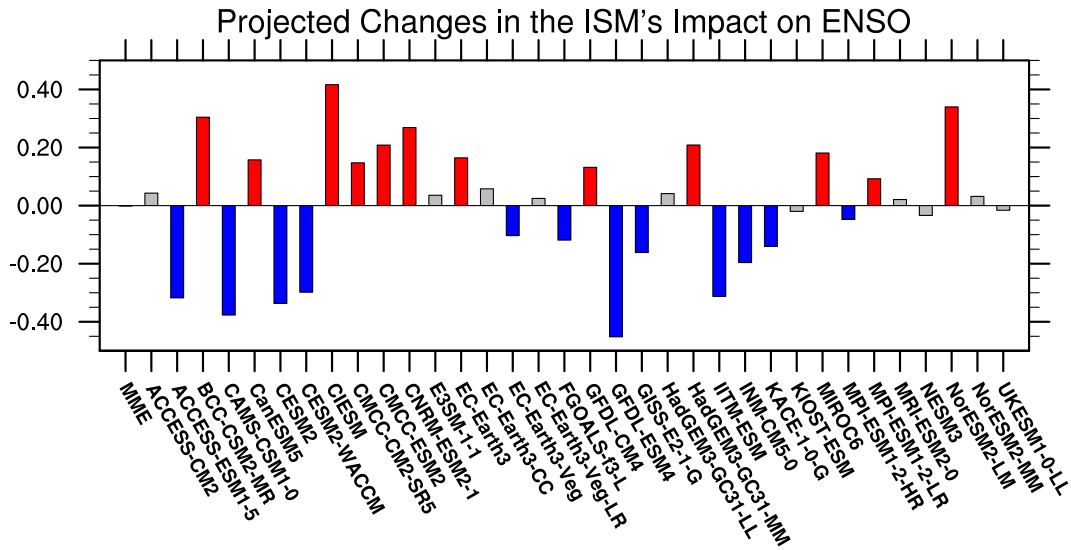


**Figure 1.** Projected changes in the strength of ISM impact on ENSO in the 34 CMIP6 models (units: °C), which are represented by changes in the monsoon-impact index. The red and blue bars highlight 12 models with the most significant positive and negative changes, categorized as strengthening-impact models and weakening-impact models, respectively.

those with a normal monsoon. For simplicity, the symmetric effects of the weak and strong monsoons on ENSO are considered. This index, referred to as monsoon-impact index (MII), is formulated as follows:

$$MII = \frac{1}{4} * ((SSTA_{EN-Dry} - SSTA_{EN-Nor}) + (SSTA_{EN-Nor} - SSTA_{EN-Wet}) + (SSTA_{LN-Dry} - SSTA_{LN-Nor}) + (SSTA_{LN-Nor} - SSTA_{LN-Wet})),$$

which is further simplified as

$$MII = \frac{(SSTA_{EN-Dry} - SSTA_{EN-Wet}) + (SSTA_{LN-Dry} - SSTA_{LN-Wet})}{4},$$

where the $SSTA_{EN-Dry}$ represents the October–December (OND) mean Niño3.4 SST anomaly in EN-Dry years and so on. The larger the index, the stronger the monsoon's influence on the following ENSO SST anomalies, and vice versa. It should be emphasized that, because the MII only considers the symmetric feature of the monsoon's impact on ENSO, it may be misleadingly similar in mathematical form to a simpler index, which is based on the SST anomaly difference between weak and strong monsoon events (i.e., $SSTA_{Dry}$ minus $SSTA_{wet}$). However, there is a fundamental distinction between the two. The difference between dry and wet monsoon years inherently includes a significant portion of ENSO signals (i.e., resembling La Niña minus El Niño), thus making it difficult to isolate the component of anomalies attributable to the monsoon (Lin et al., 2023; R. Wu & Kirtman, 2003). In contrast, the conditional approach facilitates a more precise separation of the anomalies induced by the ISM under El Niño and La Niña conditions, thereby providing a clearer depiction of the monsoon's influence on ENSO.

## 3. Results

### 3.1. Intermodel Spread in the Projections of ISM's Effects on ENSO

Figure 1 shows the projected changes in the MII for the SSP585 simulations (2015–2099) relative to the historical simulations (1900–2014) in the 34 CMIP6 models. There is prominent uncertainty in the future projections of the ISM influences on ENSO. Nearly half of the models simulate an enhancing impact of ISM on ENSO under global warming, whereas the other half suggests a weakening effect. The MME of the 34 models shows almost no change in the MII due to the large spread in the projections across the models.

Then, what could be the main source of such diverse changes in the influence of monsoon on ENSO across the CMIP6 models? To answer this question, we select two groups of models for comparison. One group includes the 12 models that simulate the most significant strengthening of monsoon influences on ENSO (red bars; Figure 1), referred to as the strengthening-impact models (SIMs). The other consists of the 12 models projecting the largest negative changes in the MII (blue bars; Figure 1), referred to as the weakening-impact models (WIMs). Figure 2 illustrates the monthly evolution of Niño3.4 index during the ENSO events concurrent with either abnormal or normal monsoon conditions during their developing summer in both historical and SSP585 simulations for the two groups of models. For SIMs, it is notable that the differences in Niño3.4 index between El Niño events coinciding with a dry or wet ISM and those with normal monsoon are more pronounced in the SSP585 simulations than the historical simulations (Figures 2a and 2c), particularly for the months following the monsoon season. This feature indicates that both the positive effect of weak ISMs and the negative effect of strong ISMs on El Niño development are projected to intensify under global warming. Similarly, these models also project an enhancing influence of abnormal monsoons on the following La Niña evolution (Figures 2b and 2d). In contrast, the SST differences between ENSO events concurrent with and without abnormal monsoons diminish and become insignificant in the SSP585 simulations of WIMs, suggesting that WIMs project a notable weakening of the monsoon effects on ENSO (Figures 2e–2h). This result further demonstrates the substantial differences in the projected changes in the ISM's influences on ENSO development between the two groups of CMIP6 models, which also validate the findings shown in Figure 1.

### 3.2. Causes of the Intermodel Spread in CMIP6 Projections

To further investigate the potential causes of the divergence in projections of ISM impacts on ENSO across the CMIP6 models, we analyze the physical processes involved in the monsoon's effects on ENSO in the two groups of models. Figure 3 depicts the MME of composite differences in precipitation, 850-hPa winds, and SST anomalies during JJAS and OND between EN-Dry and EN-Nor events in both historical and SSP585 simulations for SIMs. In the EN-Dry years, ISM rainfall significantly decreases relative to the EN-Nor years with increased rainfall and anomalous cyclonic circulation over the tropical NWP (Figure 3a). As a result, anomalous westerly winds appear over the western equatorial Pacific along the southern edge of the cyclonic circulation. Lin et al. (2023) have proposed the mechanisms by which anomalous ISMs induce anomalous rainfall and circulation over the tropical NWP, subsequently influencing the following ENSO evolution. Specifically, the negative diabatic heating anomaly associated with weaker-than-normal monsoon precipitation can trigger an atmospheric cold Kelvin wave propagating eastward, leading to anomalous westerly winds over the Indo-Pacific region (Figure 3a). Especially over the western Pacific, the anomalous westerly winds are strongest at the equator and diminish with increasing latitude, leading to low-level cyclonic wind shear. The wind shear induces anomalous convergence in the atmospheric boundary layer over the tropical NWP via the Ekman pumping, thus enhancing the local precipitation (B. Wu et al., 2009; Xie et al., 2009). Then, the increased precipitation, in turn, stimulates the atmospheric Rossby wave with anomalous cyclonic circulation. This feedback between precipitation and circulation is key to the development of anomalous cyclonic circulation. The anomalous westerly winds on the southern side of the cyclonic circulation then modulate the ongoing El Niño development by triggering oceanic equatorial downwelling Kelvin waves and by facilitating the eastward movement of warm water (Figure 3g) (Lin et al., 2023). The atmosphere-ocean coupling over the equatorial Pacific exhibits the strongest magnitude from June to October (Galanti et al., 2002; Wengel et al., 2018). The Pacific SST perturbations caused by the ISM can be further aggravated by inducing a strong positive Bjerknes feedback (Figures 3d and 3j) (Bjerknes, 1969) consistent with intensified westerly wind anomalies over the equator that shift eastward (Figures 3a and 3d).

For SIMs, the ISM-driven positive rainfall anomalies over the tropical NWP are projected to increase in the warmer future corresponding to a strengthening of the anomalous cyclonic circulation over this region (Figures 3b and 3c). Therefore, the promoting effects of weak ISMs on the subsequent El Niño development are significantly enhanced under global warming (Figures 3g–3l). By contrast, WIMs simulate much smaller rainfall and circulation anomalies triggered by the ISM over the tropical NWP in the SSP585 simulations compared to those in the historical simulations (Figures 4a–4c). This leads to a notable reduction in the growth of El Niño SSTs during the months following JJAS for El Niño events coinciding with a weak ISM compared to those with a normal monsoon (Figures 4j–4l), indicating that WIMs project a substantial weakening of the influences of weak ISMs on El Niño in a warmer climate.

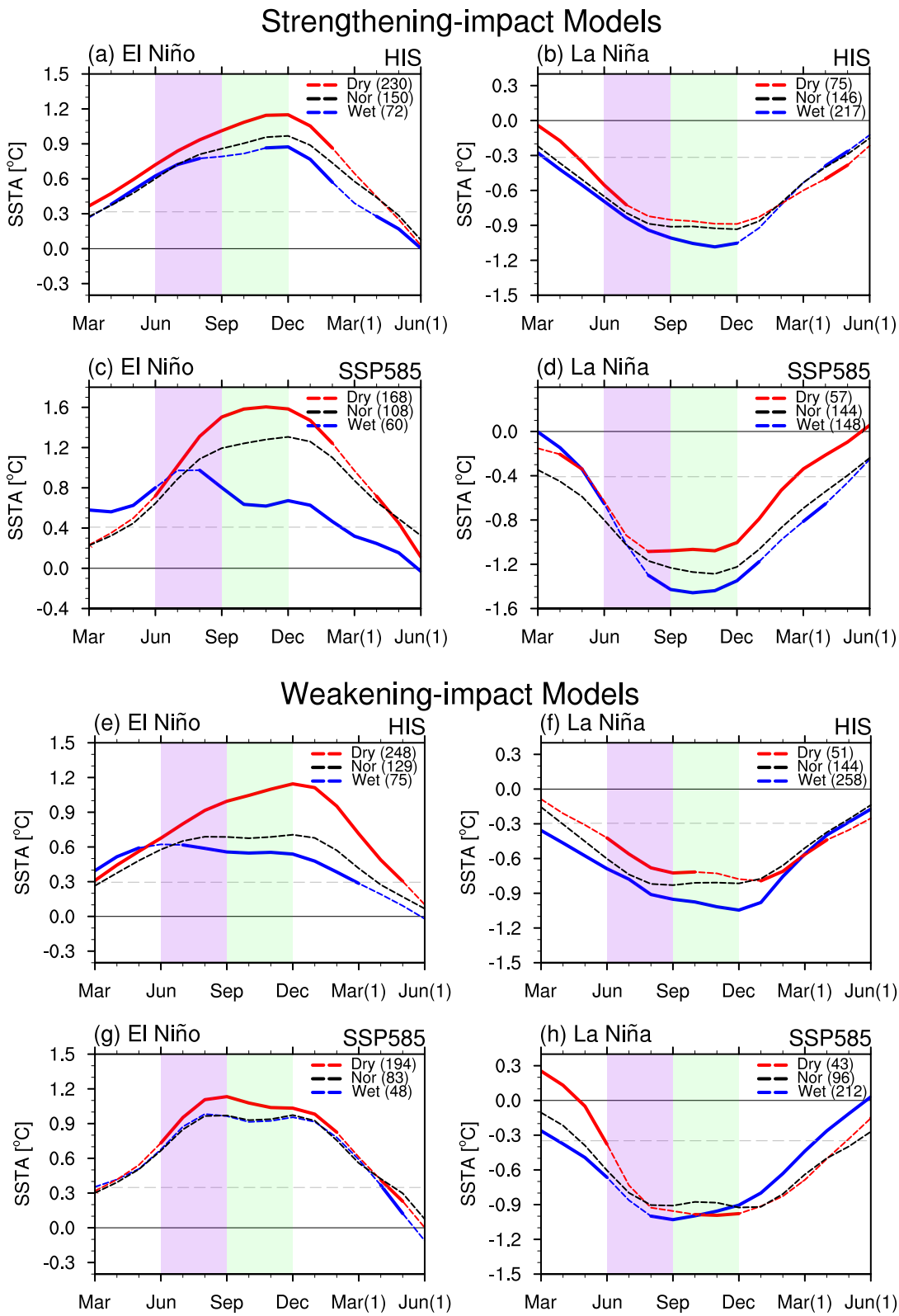


**Figure 2.**

SIMs also simulate an intensified negative influence of strong ISMs on the subsequent El Niño evolution under global warming (Figures 5j–5l), whereas WIMs project the opposite change (Figures 6j–6l). In SIMs, the decreased rainfall and anomalous anticyclone over the tropical NWP triggered by strong ISMs are projected to intensify in a warmer future (Figures 5a–5c). The corresponding easterly winds on the southern edge of the anomalous circulation are also strengthened, resulting in a more pronounced negative impact of ISMs on subsequent El Niño evolution (Figures 5j–5l). Conversely, in WIMs, both the anticyclonic circulation and negative precipitation anomalies over the tropical NWP are significantly weakened in the SSP585 simulations, leading to a weakening of anomalous winds over the western equatorial Pacific caused by ISM (Figures 6a–6c). Consequently, the anomalous monsoons exert only negligible impacts on the subsequent ENSO SST anomalies (Figures 6j–6l). These results suggest that the substantial divergence in the projected changes in the effects of ISM on El Niño between the two groups of models can be attributed to the diverse changes in the anomalous precipitation and circulation caused by ISM over the tropical NWP. We also analyze the differences between La Niña events coinciding with and without abnormal monsoons, which yield consistent results (figure not shown). It should be pointed out that, in Figures 4c, 5c, and 6c, the differences in SST and wind anomalies between SSP585 and historical simulation are evident over the subtropical northeastern Pacific during the boreal summer. Previous studies have indicated that the atmospheric and SST anomalies over the North Pacific during the preceding winter and spring, such as the North Pacific oscillation (S. Chen et al., 2024a, b), the North Pacific meridional mode (Fan et al., 2020, 2023), and the Aleutian Low (S. Chen et al., 2023), could exert significant impacts on the ENSO evolutions during the following seasons through the seasonal footprinting mechanism (Vimont et al., 2003). The changes in SST anomalies over the subtropical Pacific thus may also influence the following ENSO evolution. Nevertheless, these changes cannot explain the distinct difference in projections of the monsoon influences on ENSO between SIMs and WIMs. Although WIMs simulate a negative change in the SST differences between EN-Dry and EN-Nor years in the subtropical northeastern Pacific (Figure 4i), SIMs show a negligible change in this region (Figure 3i). Furthermore, for the differences between EN-Wet and EN-Nor years, both SIMs and WIMs simulate warmer SSTs in the subtropical Pacific rather than exhibiting opposite changes (Figures 5i and 6i). We have also examined the changes in preceding springtime SST and wind anomalies over the North Pacific and found that, consistent with the summer season, there are no significant opposite changes between the two groups of models (figure not shown).

What causes the opposite signs of the projected changes in anomalous rainfall and circulation induced by the anomalous monsoon over the NWP in the two groups of models? A straightforward hypothesis is that larger monsoon anomalies would lead to more intense anomalous circulation over the tropical NWP in a warmer future, and vice versa. In SIMs, both negative and positive precipitation anomalies indeed intensify to some extent over the India Peninsula (Figures 3c and 5c). However, the WIMs also simulate an increase in the magnitude of ISM rainfall anomaly under global warming (Figures 4c and 6c). Figure 7 shows the projected changes in the interannual variability of ISM rainfall anomalies across the 34 CMIP6 models. Nearly all models simulate an increase in the magnitude of monsoon variability in the SSP585 simulations compared to the historical simulations with WIMs showing a comparable increase to SIMs. Thus, the changes in the amplitude of monsoon anomalies do not account for the intermodel spread in the projections of ISM impacts on ENSO.

Given that the NWP precipitation-circulation feedback is also essential to the formation of ISM-induced circulation anomalies over the tropical NWP, the differences in the projected changes in the strength of this feedback may contribute to the diverse projections among the models. Even if the initial wind shear over the tropical NWP induced by the monsoon remains unchanged, the changes in the precipitation-circulation feedback could still result in distinct alterations in the response of NWP circulation to anomalous ISMs. To examine this hypothesis, we adopt the approach of X. Wang et al. (2021) and define the strength of the precipitation-circulation feedback as the regression coefficient of precipitation onto area-averaged low-level (1000–850 hPa) relative vorticity anomalies over the tropical NWP, which is shown in Figure 8. In both SIMs and WIMs, increased rainfall is related to positive low-level vorticity anomalies (i.e., cyclonic wind shear), and vice versa (Figures 8a and 8d).

**Figure 2.** Monthly evolution of Niño3.4 index for (a) El Niño and (b) La Niña events, categorized by the simultaneous occurrence of a dry (weak; red dash line), wet (strong; blue dash line), or normal monsoon (black dash line) for the historical simulations of SIMs. (c)–(d) As in (a)–(b), but for SSP585 simulations. (e)–(h) As in (a)–(d), but for WIMs. Gray dashed lines indicate 0.43 STD of the JJAS Niño3.4 index. Bold lines indicate that more than 68% of models show the same sign as the MME for the difference in the SST anomaly between ENSO events coinciding with and without abnormal monsoons. Purple shading marks the monsoon season, whereas green shading highlights the subsequent October–December period. The number of events included in the composite analysis is indicated by the values in parentheses.

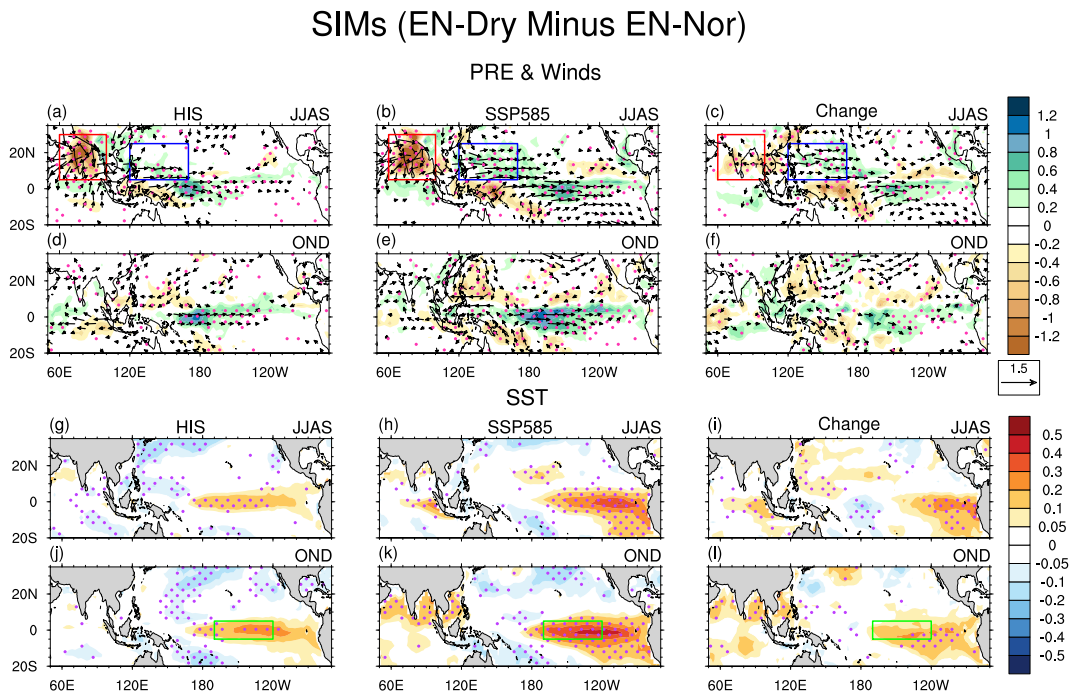


**Figure 3.** MME of differences in composite anomalies of JJAS precipitation (shading; mm day$^{-1}$) and winds at 850 hPa (vector; m s$^{-1}$) between EN-Dry and EN-Nor years in (a) the historical simulations and (b) SSP585 simulations for SIMs. (c) The differences between (a) and (b). (d)–(f) As in (a)–(c) but for OND. (g)–(l) As in (a)–(f) but for SST anomalies (shading; °C). Dotted areas indicate regions where more than 68% of the models show the same sign as the MME, whereas vectors are shown only where at least 68% of the models agree on the MME's sign. The Indian, tropical NWP, and Niño3.4 regions are highlighted by red, blue, and green boxes, respectively.

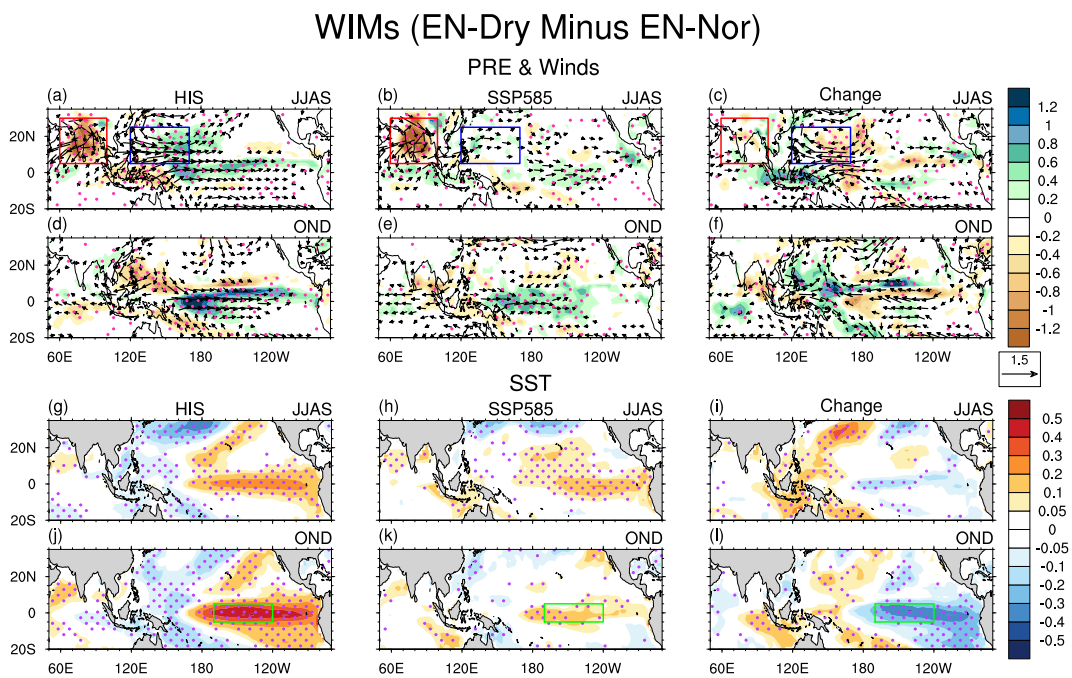


**Figure 4.** As in Figure 3, but for WIMs.

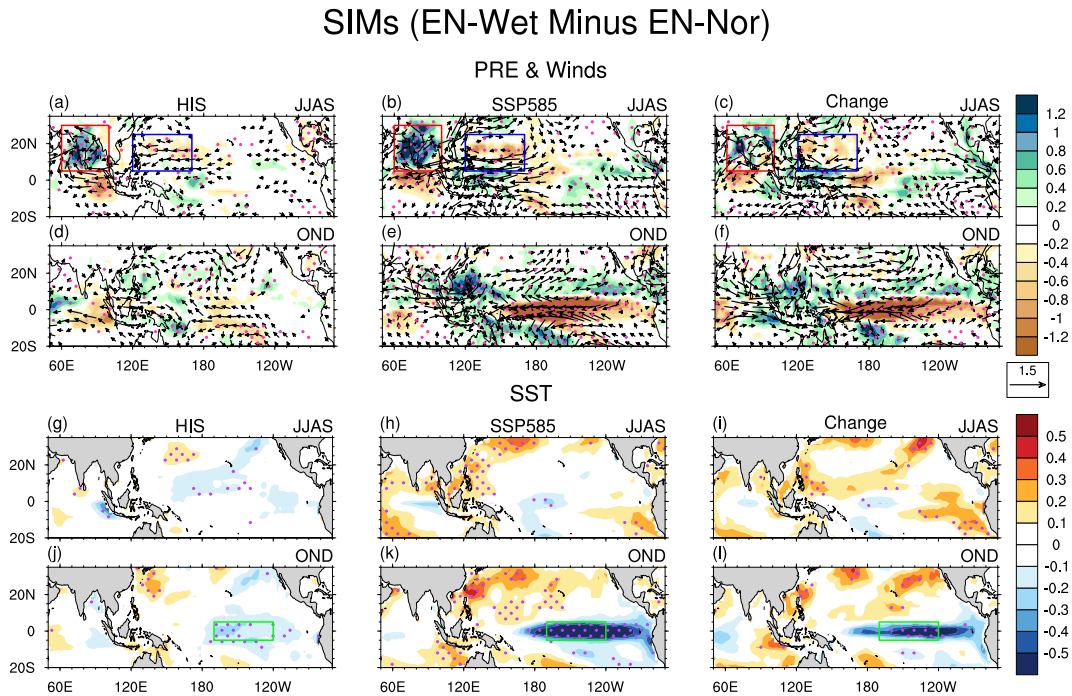


**Figure 5.** As in Figure 3, but for the differences between EN-Wet and EN-Nor years in SIMs.

The anomalous rainfall, in turn, perturbates the low-level winds by exciting the atmospheric Rossby waves, thereby establishing a positive feedback loop between the anomalous circulation and precipitation. Compared with the historical simulations, there is a prominent increase in the rainfall anomalies regressed onto low-level vorticity anomalies in the SSP585 simulations, indicating that a unit of cyclonic wind shear induced by ISMs can result in a larger increase in NWP rainfall (Figures 8b and 8c). Therefore, in SIMs the feedback between

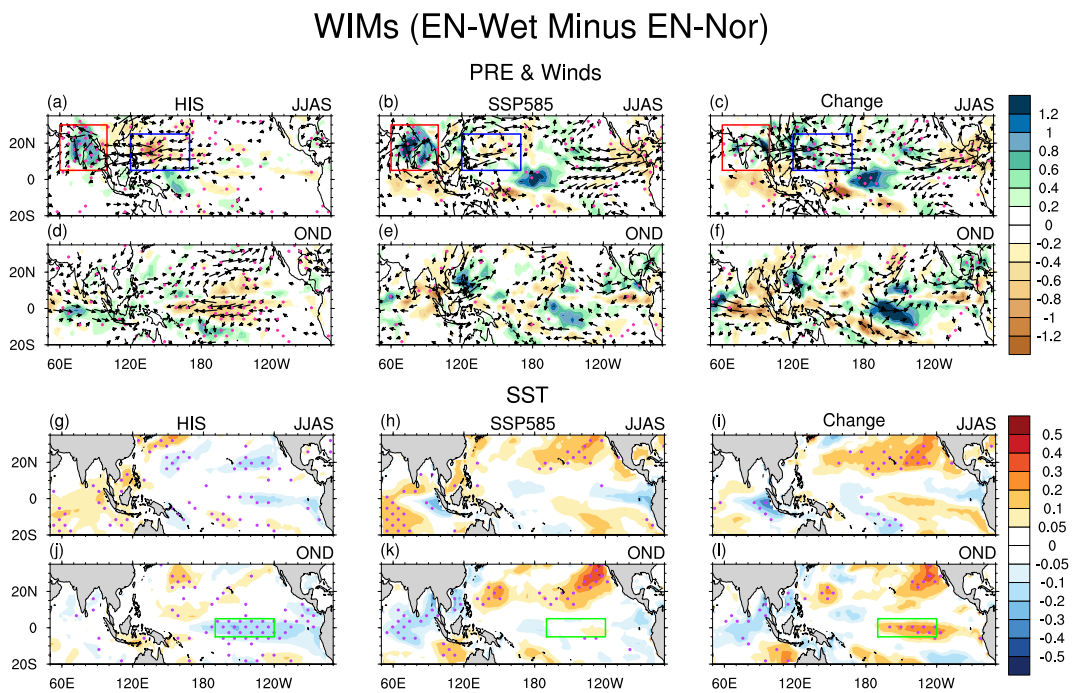


**Figure 6.** As in Figure 5, but for WIMs.

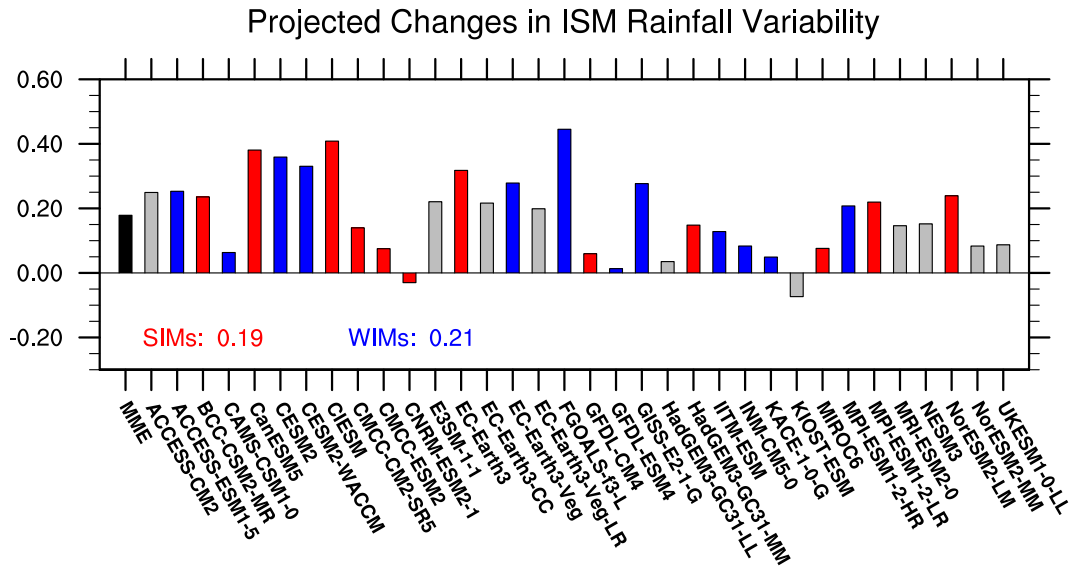


**Figure 7.** Projected changes in interannual variability of ISM rainfall anomalies (units: mm day$^{-1}$) in the 34 CMIP6 models. The results are based on the differences in the standard deviation of JJAS-mean ISM rainfall anomalies between SSP585 (2015–2099) and historical (1900–2014) simulations. Red (blue) bars highlight the SIMs (WIMs), and its MME is shown by the colored text.

precipitation and low-level circulation is expected to intensify under global warming. In contrast, WIMs project a weakening response of rainfall to anomalous low-level circulation over the tropical NWP, suggesting a diminished strength of the precipitation-circulation feedback under global warming (Figures 8e and 8f). These results reveal opposite changes in the strength of the precipitation-circulation feedback between SIMs and WIMs.

The strengths of the precipitation-circulation feedback in the CMIP6 models are further calculated by averaging the regressed precipitation anomalies over the tropical NWP. We represent a scatter plot depicting the projected changes in the precipitation-circulation feedback strength against the changes in the intensity of ISM impacts on ENSO among the models (Figure 9a). A strong positive correlation is observed between the two, indicated by a significant correlation coefficient of 0.45 (at a 99% confidence level). When the model projects enhancing

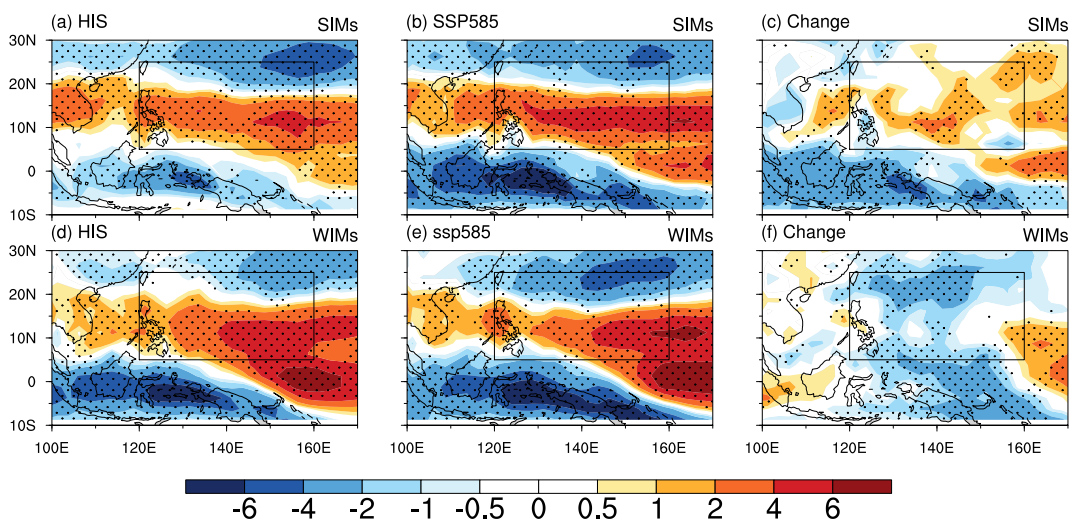


**Figure 8.** Regressed precipitation anomalies (shading; unit: $10^{-5}$ mm day$^{-1}$s$^{-1}$) onto the area-averaged low-level relatively vorticity (1000–850 hPa) over the tropical NWP (120°E–160°E, 5°N–25°N) for (a) historical simulations, (b) SSP585 simulations of SIMs. (c) The differences between (a) and (b). (d)–(f) As in (a)–(c) but for WIMs. Dotted areas indicate regions where more than 68% of the models show the same sign as the MME.

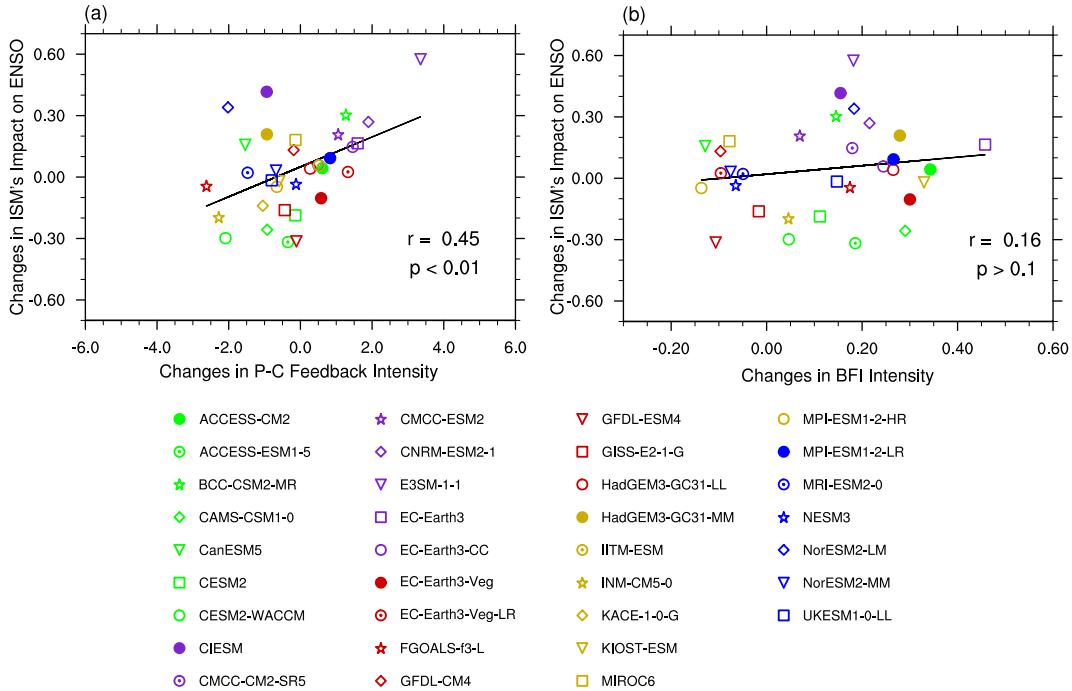


**Figure 9.** (a) Scatterplots of the projected changes in the strength of ISM impacts on ENSO and the changes in the strength of NWP precipitation-circulation feedback among 34 CMIP6 models. The precipitation-circulation feedback strength is measured by the regression coefficient linking precipitation to local relative vorticity anomalies. (b) As in (a) but for BFI. The black lines represent the linear fit. The r and p indicate the intermodel correlation and the corresponding p value, respectively.

precipitation-circulation feedback, it tends to simulate an intensified influence of the ISM on ENSO in response to global warming, and vice versa. Therefore, the diverse changes in the impacts of ISM on ENSO under global warming are tightly linked to the intermodel divergence in the projections of precipitation-circulation feedback over the tropical NWP.

Since the air-sea coupling strength over the equatorial Pacific also affects the intensity of ISM influences on ENSO (Lin et al., 2023), the diverse changes in this coupling strength may dominate the intermodel spread in the projections of the ISM effects on ENSO across the models. A unit of anomalous zonal winds caused by the monsoon over the western Pacific could induce larger SST anomalies in the central-eastern equatorial Pacific after the monsoon season under intensified Pacific air-sea coupling. To explore this possibility, we further calculate the changes in the Bjerknes feedback intensity (BFI). The BFI indicates the air-sea coupling strength over the tropical Pacific, involving three processes: the response of surface winds to SST variation, the effect of surface winds on thermocline depth, and the response of SST to changes in thermocline depth (Bjerknes, 1969; L. Chen et al., 2015; Liu et al., 2011). A detailed explanation about how the BFI is calculated can be referred to Text S1 in Supporting Information S1. The projected change in BFI shows a weak intermodel correlation with the change in the strength of monsoon effects on ENSO across the models (Figure 5b). Therefore, the intermodel spread in the projections of ISM influences on ENSO is mainly attributed to the variations in the intensity of NWP precipitation-circulation feedback rather than the changes in Pacific air-sea coupling strength.

## 4. Conclusion and Discussion

This study investigates the projected changes in the ISM's impacts on ENSO under global warming using 34 CMIP6 models that exhibit plausible skills in representing the influences of ISM on ENSO during the historical period. It is found that there exists a pronounced intermodel spread in the projections: nearly half of the models simulate a strengthening influence of the monsoon on ENSO, whereas the others suggest a weakening impact. This diversity results in the MME of the 34 models showing a negligible change in this regard under global warming. The key factors behind the diverse projections are examined by comparing the results of two groups of

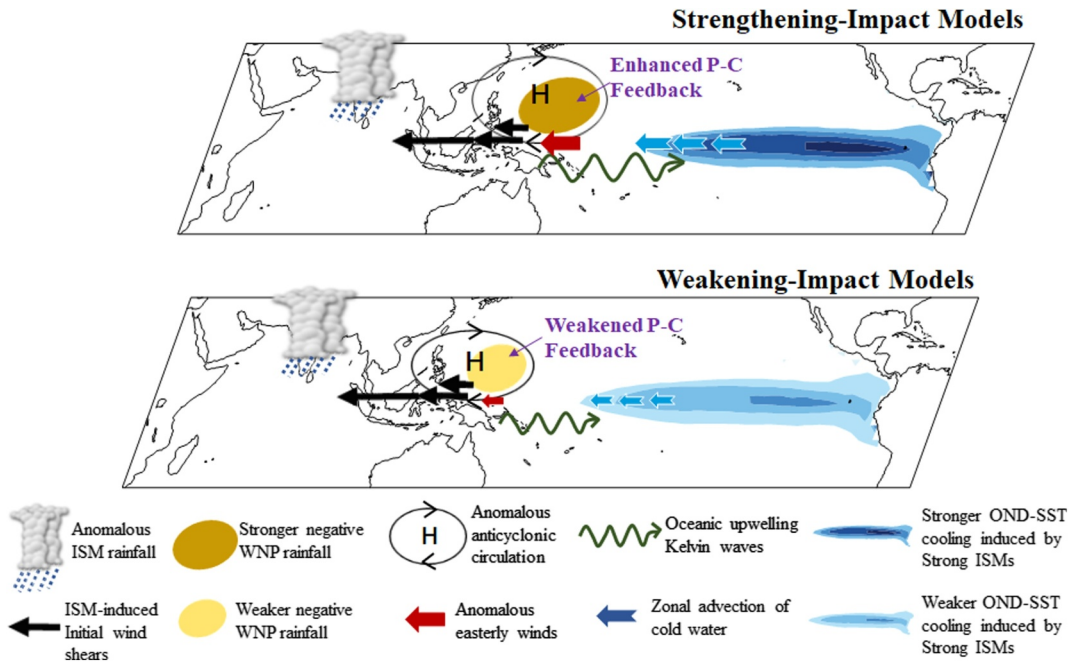


**Figure 10.** Schematic diagram depicting the causes of intermodel spread in the CMIP6 projections of ISM impacts on ENSO.

models: the strengthening-impact models (SIMs) and the weakening-impact models (WIMs), which are summarized in Figure 10.

In SIMs, both weaker- and stronger-than-normal monsoons are projected to exert more pronounced impacts on ENSO evolution in the SSP585 simulations relative to the historical simulations. This intensification is attributed to the strengthening of ISM-driven anomalous precipitation and circulation over the tropical NWP. The enhancing anticyclonic (cyclonic) circulation induced by strong (weak) ISMs corresponds to stronger anomalous easterly (westerly) winds on its southern side, which suppress (amplify) the positive feedback processes essential for El Niño development more significantly, thereby intensifying the ISM's effects on the subsequent ENSO evolution. In contrast, WIMs project a diminished influence of ISM on ENSO under global warming due to the weakening of rainfall and circulation over the tropical NWP caused by the monsoon. Further investigations reveal that the divergence in the model projections is closely related to the changes in the feedback strength between precipitation and low-level circulation over the tropical NWP. Models that project strengthening precipitation-circulation feedback tend to simulate an increase in ISM-induced rainfall and circulation anomaly. This is because the ISM-induced initial wind shear over the tropical NWP is more effective in generating rainfall anomalies and resultant anomalous cyclonic or anticyclonic circulation under the stronger local precipitation-circulation feedback. However, in WIMs, the feedback strength is expected to weaken considerably, reducing the ability of ISM-induced wind shear to effectively generate anomalous rainfall and circulation over the NWP. As a result, the influence of the ISM on ENSO is projected to weaken in the context of global warming in WIMs.

This study highlights the critical role of NWP precipitation-circulation feedback in determining the intermodel spread in the projections of ISM impacts on ENSO across the CMIP6 models. Improving the projections of this feedback might contribute to reducing the uncertainties in projecting the ENSO-ISM relationship under global warming. The potential causes for the diverse changes in the precipitation-circulation feedback among CMIP6 models need to be further discussed. Previous studies have suggested that higher mean moisture favors a larger intensity of convection-circulation feedback (He et al., 2017; Xie et al., 2009). Anomalous low-level winds tend to induce larger precipitation perturbation under higher background mean moisture. The larger rainfall anomaly in turn could strengthen the anomalous circulation through releasing more condensational heating. We analyzed the projected changes in surface mean moisture over the tropical NWP in both SIMs and WIMs and found that the mean moisture would increase in response to global warming in the two groups of models (figure not shown). The changes in mean moisture thus cannot account for the different changes in precipitation-circulation feedback

strength between the two groups of models. In fact, as highlighted by prior studies (Luo et al., 2024; Z. Wang et al., 2024; Yan et al., 2020), precipitation anomalies in the tropics are influenced not only by moisture but also by atmospheric circulation with a strong association with moisture transport driven by anomalous vertical motions. The projected changes in regressed precipitation anomaly onto low-level vorticity anomaly can be decomposed as $\Delta P' \sim -\left(\Delta\overline{q} * \dot{w}_{his} + \overline{q}_{his} * \Delta w'\right)$ (Huang & Xie, 2015), where $\Delta P'$ represents the changes in regressed precipitation anomaly, $\overline{q}$ and $w'$ denote the climatological near-surface specific humidity and regressed vertical velocity anomaly at 500hpa onto low-level vorticity anomaly, respectively. $\Delta$ represents the difference between the historical and SSP585 simulations. Projected changes in the feedback strength between precipitation and low-level horizontal circulation are thus dominated by the changes in both mean moisture and the coupling between vertical motion and low-level horizontal circulation. Figure S3 in Supporting Information S1 shows the decomposition of the projected changes in precipitation anomalies regressed onto the NWP low-level relative vorticity. Although the increased mean moisture under global warming favors larger rainfall anomalies over the NWP in both SIMs and WIMs, the changes in the coupling strength between vertical motions and low-level circulation show opposite changes between SIMs and WIMs with larger magnitudes. Thus, the diverse changes in the precipitation-circulation feedback over the tropical NWP can be further attributed to the changes in the coupling strength between anomalous horizontal circulation and vertical motions. As suggested by the moist enthalpy advection mechanism, this coupling could be related to the moist static energy transported by the anomalous horizontal circulation (B. Wu et al., 2017). Therefore, the changes in this coupling strength might be linked to the variations in the energy transported by anomalous low-level circulation. In addition, the changes in atmospheric static stability under global warming might also influence the response of vertical motions to anomalous moist static energy transport or diabatic heating (Huang et al., 2017; Y. Wang et al., 2020). Further investigations are required to elucidate the influences of these factors.

## Conflict of Interest

The authors declare no conflicts of interest relevant to this study.

## Data Availability Statement

The HadISST data set is available at the website of the UK Met Office (https://www.metoffice.gov.uk/hadobs/hadisst/), and the AIMR data set was obtained from https://tropmet.res.in/data/data-archival/rain/iitm-regionrf.txt. The CMIP6 models utilized in this work are detailed in Table S1 in Supporting Information S1 and preserved at Lin (2025), and the model outputs were downloaded from the Earth System Grid Federation (https://esgf-node.llnl.gov/search/cmip6/).

**Acknowledgments**
The authors thank the three anonymous reviewers who provided constructive comments on the earlier version of this paper. This work was supported by the National Natural Science Foundation of China (42088101), the Innovation Group Project of Southern Marine Science and Engineering Guangdong Laboratory (Zhuhai) (316323005), the Guangdong Province Key Laboratory for Climate Change and Natural Disaster Studies (2023B1212060019), and the Geography Postdoctoral Programs at Fujian Normal University.

## References

Aneesh, S., & Bódai, T. (2024). Inter-model robustness of the forced change of the ENSO-Indian summer monsoon teleconnection. *NPJ Climate and Atmospheric Science*, *7*(1), 4. https://doi.org/10.1038/s41612-023-00541-w

Annamalai, H., Hamilton, K., & Sperber, K. R. (2007). The South Asian summer monsoon and its relationship with ENSO in the IPCC AR4 simulations. *Journal of Climate*, *20*(6), 1071–1092. https://doi.org/10.1175/JCLI4035.1

Bjerknes, J. (1969). Atmospheric teleconnections from the equatorial Pacific. *Monthly Weather Review*, *97*(3), 163–172. https://doi.org/10.1175/1520-0493(1969)097<0163:atftep>2.3.co;2

Chen, J., Yang, S., Fang, X., Lin, S., Pérez-Carrasquilla, J. S., Cai, F., et al. (2024). A novel index for depicting ENSO transition with application in ENSO-East Asian summer monsoon relationship. *Environmental Research Letters*, *19*(12), 124066. https://doi.org/10.1088/1748-9326/ad9290

Chen, L., Li, T., & Yu, Y. (2015). Causes of strengthening and weakening of ENSO amplitude under global warming in four CMIP5 models. *Journal of Climate*, *28*(8), 3250–3274. https://doi.org/10.1175/JCLI-D-14-00439.1

Chen, S., Chen, W., Xie, S. P., Yu, B., Wu, R., Wang, Z., et al. (2024a). Strengthened impact of boreal winter North Pacific Oscillation on ENSO development in warming climate. *NPJ Climate and Atmospheric Science*, *7*(1), 1–11. https://doi.org/10.1038/s41612-024-00615-3

Chen, S., Chen, W., Yu, B., Wu, R., Graf, H. F., & Chen, L. (2023). Enhanced impact of the Aleutian low on increasing the central Pacific ENSO in recent decades. *NPJ Climate and Atmospheric Science*, *6*(1), 1–13. https://doi.org/10.1038/s41612-023-00350-1

Chen, S., Chen, W., Zhou, W., Wu, R., Ding, S., Chen, L., et al. (2024b). Interdecadal variation in the impact of Arctic Sea Ice on El Niño–southern oscillation: The role of atmospheric mean flow. *Journal of Climate*, *37*(21), 5483–5506. https://doi.org/10.1175/JCLI-D-23-0733.1

Chowdary, J. S., Xie, S.-P., & Nanjundiah, R. S. (2021). Chapter 1 - Drivers of the Indian summer monsoon climate variability. In J. Chowdary, A. Parekh, & C. Gnanaseelan (Eds.), *Indian summer monsoon variability* (pp. 1–28). Elsevier. https://doi.org/10.1016/B978-0-12-822402-1.00020-X

Chung, C., & Nigam, S. (1999). Asian summer monsoon-ENSO feedback on the Cane-Zebiak model ENSO. *Journal of Climate*, *12*(9), 2787–2807. https://doi.org/10.1175/1520-0442(1999)012<2787:ASMEFO>2.0.CO;2

Eyring, V., Bony, S., Meehl, G. A., Senior, C. A., Stevens, B., Stouffer, R. J., & Taylor, K. E. (2016). Overview of the coupled model Intercomparison project phase 6 (CMIP6) experimental design and organization. *Geoscientific Model Development*, *9*(5), 1937–1958. https://doi.org/10.5194/GMD-9-1937-2016

Fan, H., Huang, B., Yang, S., & Dong, W. (2020). Influence of the Pacific meridional mode on ENSO evolution and predictability: Asymmetric modulation and ocean preconditioning. *Journal of Climate*, *34*(5), 1881–1901. https://doi.org/10.1175/jcli-d-20-0109.1

Fan, H., Yang, S., Wang, C., & Lin, S. (2023). Revisiting the impacts of tropical Pacific SST anomalies on the Pacific meridional mode during the decay of strong eastern Pacific El Niño events. *Journal of Climate*, *36*(15), 4987–5002. https://doi.org/10.1175/JCLI-D-22-0342.1

Fang, K., Mei, Z., Wu, H., Zhou, F., Seppä, H., & Guo, Z. (2024). Indian summer monsoon drives synchronous interdecadal hydroclimate changes in the Tibetan Plateau and surroundings. *Global and Planetary Change*, *234*, 104379. https://doi.org/10.1016/j.gloplacha.2024.104379

Galanti, E., Tziperman, E., Harrison, M., Rosati, A., Giering, R., & Sirkes, Z. (2002). The equatorial thermocline outcropping-A seasonal control on the tropical Pacific ocean-atmosphere instability strength. *Journal of Climate*, *15*(19), 2721–2739. https://doi.org/10.1175/1520-0442(2002)015<2721:tetoas>2.0.co;2

Goswami, B. B., & An, S.-I. (2022). An assessment of the ENSO-monsoon teleconnection in a warming climate. *NPJ Climate and Atmospheric Science*, *6*(82), 1–10. https://doi.org/10.21203/rs.3.rs-2101241

He, C., Lin, A., Gu, D., Li, C., & Zheng, B. (2017). Formation mechanism for the amplitude of interannual climate variability in subtropical northern hemisphere: Relative contributions from the zonal asymmetric mean state and the interannual variability of SST. *Climate Dynamics*, *48*(1–2), 697–705. https://doi.org/10.1007/s00382-016-3105-8

Huang, P., Chen, D., & Ying, J. (2017). Weakening of the tropical atmospheric circulation response to local sea surface temperature anomalies under global warming. *Journal of Climate*, *30*(20), 8149–8158. https://doi.org/10.1175/JCLI-D-17-0171.1

Huang, P., & Xie, S. (2015). Mechanisms of change in ENSO-induced tropical Pacific rainfall variability in a warming climate. *Nature Geoscience*, *8*(October), 922–926. https://doi.org/10.1038/NGEO2571

Ju, J., & Slingo, J. (1995). The Asian summer monsoon and ENSO. *Quarterly Journal of the Royal Meteorological Society*, *121*(525), 1133–1168. https://doi.org/10.1002/qj.49712152509

Kinter, I. L., Miyakoda, K., & Yang, S. (2002). Recent change in the connection from the Asian monsoon to ENSO. *Journal of Climate*, *15*(10), 1203–1215. https://doi.org/10.1175/1520-0442(2002)015<1203:RCITCF>2.0.CO;2

Kirtman, B. P., & Shukla, J. (2000). Influence of the Indian summer monsoon on ENSO. *Quarterly Journal of the Royal Meteorological Society*, *126*(562), 213–239. https://doi.org/10.1002/qj.49712656211

Kumar, K. K., Rajagopalan, B., & Cane, M. A. (1999). On the weakening relationship between the Indian monsoon and ENSO. *Science*, *284*(5423), 2156–2159. https://doi.org/10.1126/science.284.5423.2156

Kumar, K. K., Rajagopalan, B., Hoerling, M., Bates, G., & Cane, M. (2006). Unraveling the mystery of Indian monsoon failure during El Niño. *Science*, *314*(5796), 115–119. https://doi.org/10.1126/science.1131152

Lau, K. M., & Yang, S. (1996). The Asian monsoon and predictability of the tropical ocean-atmosphere system. *Quarterly Journal of the Royal Meteorological Society*, *122*(532), 945–957. https://doi.org/10.1256/smsqj.53207

Li, X., & Ting, M. (2015). Recent and future changes in the Asian monsoon-ENSO relationship: Natural or forced? *Geophysical Research Letters*, *42*(9), 3502–3512. https://doi.org/10.1002/2015GL063557

Lin, S. (2025). Data from: Deciphering the intermodel spread in projections of the impacts of Indian summer monsoon on ENSO under global warming. *Zenodo*. https://doi.org/10.5281/ZENODO.14759313

Lin, S., Dong, B., & Yang, S. (2024a). Enhanced impacts of ENSO on the Southeast Asian summer monsoon under global warming and associated mechanisms. *Geophysical Research Letters*, *51*, e2023GL106437. https://doi.org/10.1029/2023GL106437

Lin, S., Dong, B., Yang, S., & Zhang, T. (2024b). Diverse impacts of the Indian summer monsoon on ENSO among CMIP6 models and its possible causes. *Environmental Research Letters*, *19*(8), 084052. https://doi.org/10.1088/1748-9326/ad6618

Lin, S., Yang, S., He, S., Fan, H., Chen, J., Dong, W., et al. (2023). Atmospheric–oceanic processes over the Pacific involved in the effects of the Indian summer monsoon on ENSO. *Journal of Climate*, *36*(17), 6021–6043. https://doi.org/10.1175/JCLI-D-22-0822.1

Liu, L., Yu, W., & Li, T. (2011). Dynamic and thermodynamic air-sea coupling associated with the Indian Ocean dipole diagnosed from 23 WCRP CMIP3 models. *Journal of Climate*, *24*(18), 4941–4958. https://doi.org/10.1175/2011jcli4041.1

Luo, H., Wang, Z., He, C., Chen, D., & Yang, S. (2024). Future changes in South Asian summer monsoon circulation under global warming: Role of the Tibetan Plateau latent heating. *NPJ Climate and Atmospheric Science*, *7*(1), 103. https://doi.org/10.1038/s41612-024-00653-x

Meehl, G. A. (1997). The South Asian monsoon and the tropospheric biennial oscillation. *Journal of Climate*, *10*(8), 1921–1943. https://doi.org/10.1175/1520-0442(1997)010<1921:TSAMAT>2.0.CO;2

Nigam, S. (1994). On the dynamical basis for the Asian summer monsoon rainfall-El Niño relationship. *Journal of Climate*, *7*(11), 1750–1771. https://doi.org/10.1175/1520-0442(1994)007<1750:OTDBFT>2.0.CO;2

Parthasarathy, B., Munot, A. A., & Kothawale, D. R. (1994). All-India monthly and seasonal rainfall series: 1871–1993. *Theoretical and Applied Climatology*, *49*(4), 217–224. https://doi.org/10.1007/BF00867461

Power, S. B., Delage, F., Colman, R., & Moise, A. (2012). Consensus on twenty-first-century rainfall projections in climate models more widespread than previously thought. *Journal of Climate*, *25*(11), 3792–3809. https://doi.org/10.1175/JCLI-D-11-00354.1

Rasmusson, E. M., & Carpenter, T. H. (1983). The relationship between eastern equatorial Pacific sea surface temperatures and rainfall over India and Sri Lanka. *Monthly Weather Review*, *111*(3), 517–528. https://doi.org/10.1175/1520-0493(1983)111<0517:TRBEEP>2.0.CO;2

Rayner, N. A., Parker, D. E., Horton, E. B., Folland, C. K., Alexander, L. V., Rowell, D. P., et al. (2003). Global analyses of sea surface temperature, sea ice, and night marine air temperature since the late nineteenth century. *Journal of Geophysical Research*, *108*(14), 4407. https://doi.org/10.1029/2002jd002670

Vimont, D. J., Wallace, J. M., & Battisti, D. S. (2003). The seasonal footprinting mechanism in the Pacific: Implications for ENSO. *Journal of Climate*, *16*(16), 2668–2675. https://doi.org/10.1175/1520-0442(2003)016<2668:TSFMIT>2.0.CO;2

Wang, B., Wu, R., & Lau, K.-M. (2001). Interannual variability of the Asian summer monsoon: Contrasts between the Indian and the western North Pacific-East Asian monsoons. *Journal of Climate*, *14*(20), 4073–4090. https://doi.org/10.1175/1520-0442(2001)014<4073:ivotas>2.0.co;2

Wang, X., Li, T., & He, C. (2021). Impact of the mean state on El Niño–induced western North Pacific anomalous anticyclones during El Niño decaying summer in AMIP models. *Journal of Climate*, *34*(22), 9201–9249. https://doi.org/10.1175/JCLI-D-20-0747.1

Wang, Y., He, C., & Li, T. (2020). Impact of global warming on the western North Pacific circulation anomaly during developing El Niño. *Journal of Climate*, *33*(6), 2333–2349. https://doi.org/10.1175/JCLI-D-19-0588.1

Wang, Z., Xu, J., Zeng, Z., Ke, M., & Feng, X. (2024). Understanding the 2022 extreme Dragon-Boat Rainfall in South China from the combined land and oceanic forcing. *Asia-Pacific Journal of Atmospheric Sciences*, *60*, 1–14. https://doi.org/10.1007/s13143-024-00356-6

Webster, P. J., & Yang, S. (1992). Monsoon and ENSO: Selectively interactive systems. *Quarterly Journal of the Royal Meteorological Society*, *118*(507), 877–926. https://doi.org/10.1002/qj.49711850705

Wengel, C., Latif, M., Park, W., Harlaß, J., & Bayr, T. (2018). Seasonal ENSO phase locking in the Kiel Climate Model: The importance of the equatorial cold sea surface temperature bias. *Climate Dynamics*, *50*(3–4), 901–919. https://doi.org/10.1007/s00382-017-3648-3

Wu, B., Zhou, T., & Li, T. (2009). Seasonally evolving dominant interannual variability modes of East Asian climate. *Journal of Climate*, *22*(11), 2992–3005. https://doi.org/10.1175/2008JCLI2710.1

Wu, B., Zhou, T., & Li, T. (2017). Atmospheric dynamic and thermodynamic processes driving the western North Pacific anomalous anticyclone during El Niño. Part I: Maintenance mechanisms. *Journal of Climate*, *30*(23), 9621–9635. https://doi.org/10.1175/JCLI-D-16-0489.1

Wu, R., & Kirtman, B. P. (2003). On the impacts of the Indian summer monsoon on ENSO in a coupled GCM. *Quarterly Journal of the Royal Meteorological Society*, *129*(595 PART B), 3439–3468. https://doi.org/10.1256/qj.02.214

Xie, S. P., Hu, K., Hafner, J., Tokinaga, H., Du, Y., Huang, G., & Sampe, T. (2009). Indian Ocean capacitor effect on Indo-western Pacific climate during the summer following El Niño. *Journal of Climate*, *22*(3), 730–747. https://doi.org/10.1175/2008JCLI2544.1

Yan, Z., Wu, B., Li, T., Collins, M., Clark, R., Zhou, T., et al. (2020). Eastward shift and extension of ENSO-induced tropical precipitation anomalies under global warming. *Science Advances*, *6*(2), 1–11. https://doi.org/10.1126/sciadv.aax4177

Yang, S., Chen, D., & Deng, K. (2024). Global effects of climate change in the South China Sea and adjacent regions. *Ocean-Land-Atmosphere Research*, *3*, 0038. https://doi.org/10.34133/olar.0038

Yang, S., Deng, K., & Duan, W. (2018). Selective interaction between monsoon and ENSO: Effects of annual cycle and spring predictability barrier. *Chinese Journal of Atmospheric Sciences*, *42*(3), 570–589. https://doi.org/10.3878/j.issn.1006-9895.1712.17241

Yang, S., Li, Z., Yu, J. Y., Hu, X., Dong, W., & He, S. (2018). El Niño-Southern Oscillation and its impact in the changing climate. *National Science Review*, *5*(6), 840–857. https://doi.org/10.1093/nsr/nwy046

Yang, X., & Huang, P. (2021). Restored relationship between ENSO and Indian summer monsoon rainfall around 1999/2000. *Innovation (China)*, *2*(2), 100102. https://doi.org/10.1016/j.xinn.2021.100102

Yasunari, T. (1990). Impact of Indian monsoon on the coupled atmosphere/ocean system in the tropical Pacific. *Meteorology and Atmospheric Physics*, *44*(1–4), 29–41. https://doi.org/10.1007/BF01026809

Zhang, R., Sumi, A., & Kimoto, M. (1996). Impact of El Niño on the East Asian monsoon: A diagnostic study of the '86/87 and '91/92 events. *Journal of the Meteorological Society of Japan*, *74*(1), 49–62. https://doi.org/10.2151/jmsj1965.74.1_49